Applied Surface Science 276 (2013) 95–100

Contents lists available at SciVerse ScienceDirect

Applied Surface Science

journal homepage: www.elsevier.com/locate/apsusc

Design and laser fabrication of controllable non-Gaussian roughness surfaces at microscale

Tingting Luo [a], Xiaoning Liu [a], Yuhang Chen [a,*], Wenhao Huang [a], Zhe Liu [b]

[a] Department of Precision Machinery and Precision Instrumentation, University of Science and Technology of China, Hefei 230026, People's Republic of China
[b] Laboratory of Microfabrication, Institute of Physics, Chinese Academy of Sciences, Beijing 100190, People's Republic of China

ARTICLE INFO

Article history:
Received 24 November 2012
Received in revised form 8 March 2013
Accepted 8 March 2013
Available online 1 April 2013

Keywords:
Non-Gaussian roughness surface
Laser direct writing
Scanning probe microscopy

ABSTRACT

Surface structures at micro-/nano-scale have been studied in many fields for their wide range of applications. To understand the interdependences between surface structures and functional performances accurately, fabrication methods of complex structures with controllable surface parameters are crucial to be investigated. Toward this purpose, 3D non-Gaussian surfaces were designed and fabricated here. Two typical design methods were compared, which are based on Johnson translator and Pearson translator respectively. Several suggestions were provided to improve the design accuracy and efficiency. Primary roughness surfaces have been fabricated by laser direct writing. Different scanning paths and designed structures were compared to optimize the fabrication accuracy. The statistical and spectral characteristics of the fabricated roughness surfaces were demonstrated to be in accord with the designed values.

1. Introduction

Surface structures at micro-/nano-scale play an important role in various scientific fields, for example, electronics, information technology, energy, optics, tribology, biology and biomimetic [1]. Roughness surfaces have been investigated widely to understand their functional performances from various aspects. Patrikar [2] simulated roughness surfaces, providing a theoretical basis to highlight how microscopic roughness affects electronic properties of the material. Li and Zheng [3] modeled and simulated the influences of micro-/nano-scale roughness on power dissipation of waveguide inner surface. Klapetek et al. [4] calculated the scattering of rough surfaces using a graphical processing unit. Xiao et al. [5] discussed the influencing factors of contact ratio on rough surfaces at mixed lubrication condition. Furuta et al. [6] found the correlation between the roughness and droplet radius at the wetting mode transition when nano-liter scale water droplets were evaporated on surfaces with random roughness structures. Chen and Huang [7] numerically analyzed the factors affecting surface roughness evaluation by atomic force microscope (AFM). Panczyk et al. [8] studied the collisions frequency of ideal gas molecules with a rough surface. Arifvianto et al. [9] elucidated the mechanisms of surface mechanical attrition treatment to improve mechanical properties of metallic materials. Korayem and Zakeri [10] investigated the dynamic behavior of spherical micro-/nano-particles, which were pushed on rough substrates by means of an AFM. Kim et al. [11] conducted a 3D contact analysis to discuss the contact behavior of elastic/plastic solids with non-Gaussian surfaces. Minet et al. [12] presented some methods of non-Gaussian surface generation in order to study mixed lubrication of mechanical seal faces. However, for more quantitative investigations of all these underlying relations between surface structures and functional performances, specimens with well-defined surface parameters should be obtained first. The key issues are then the rational design and subsequently the precise fabrication of the designed surfaces with controllable parameters.

In designing non-Gaussian roughness surfaces, a series of random numbers should be firstly generated. Then the random numbers are translated to a non-Gaussian matrix with prescribed distribution. At last, the non-Gaussian matrix is filtered to obtain the expected roughness surfaces [11–15]. When random numbers are translated to a non-Gaussian matrix, both Johnson translator and Pearson translator can be utilized. Theoretical analyses of the two translators can be found in literature [13]. In many simulations, Johnson translator is adopted while fewer reports can be found on the non-Gaussian surface simulation based on Pearson translator [11–15]. In addition, there are almost no investigations on the comparisons of the two translators when they are applied to the non-Gaussian surface generation.

The fabrication of the irregular complex surfaces at the micro-/nano-scale is a challenge. Only a few numbers of works have addressed on this issue. Uchidate et al. [16] fabricated the 3D structures with the dimension of 60 μm × 60 μm using focused ion beam (FIB). Nemoto et al. [17] manufactured a 3D roughness standard,

* Corresponding author. Tel.: +86 551 63600214; fax: +86 551 63600214.
E-mail address: chenyh@ustc.edu.cn (Y. Chen).

0169-4332/$ – see front matter © 2013 Elsevier B.V. All rights reserved.
http://dx.doi.org/10.1016/j.apsusc.2013.03.040

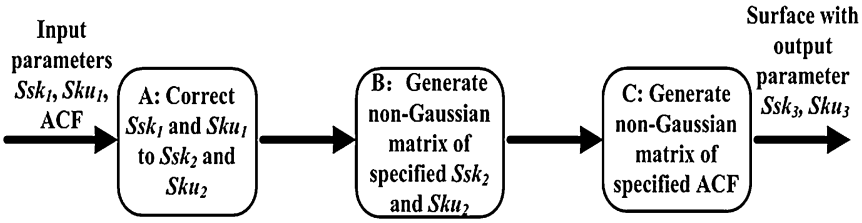

Fig. 1. Flowchart of the non-Gaussian surface generation.

whose dimension is 768 μm × 768 μm, by a super 5-axis nano-machine. Liu et al. [18] prepared a 3D reference structure with the dimension of 10 μm × 10 μm using electron beam lithography (EBL). Brissonneau et al. [19] proposed an experimental method to create Gaussian random surfaces on silicon by laser processing followed by etching. Generally, fabrications of roughness surfaces with controllable parameters, especially non-Gaussian distributed surfaces, still need to be further developed.

In this paper, non-Gaussian roughness surfaces at the micro-scale were designed and precisely fabricated. Advantages and disadvantages were compared between two typical design methods, which are based on Johnson and Pearson translators, respectively. Several suggestions were provided to improve the design accuracy and efficiency. Finally, non-Gaussian surfaces were fabricated by laser direct writing (LDW) and measured by AFM. Two typical scanning paths and three fabrication structures were designed and optimized. Both surface parameter evaluations and template matching analyses of the fabricated roughness surfaces were carried out. Results demonstrate that LDW is reliable to fabricate 3D roughness surfaces.

2. Simulation

2.1. Non-Gaussian surface generation

The flowchart of simulation is shown in Fig. 1. The input parameters are skewness (Ssk_1), kurtosis (Sku_1) and correlation length, while the output is a non-Gaussian surface with certain parameters (Ssk_3 and Sku_3). Ssk_2 and Sku_2 are the skewness and kurtosis after the modification process of Ssk_1 and Sku_1. Generally, the simulation of non-Gaussian surface consists of three modules. In module A, the modification of skewness and kurtosis of the input random sequence is applied, which can be referred to [13,14,17,18]. In module B, a non-Gaussian matrix with modified skewness and kurtosis is generated, both Johnson translator and Pearson translator can be used in this part. In module C, the non-Gaussian surface with a defined autocorrelation function (ACF) is obtained by filtering the non-Gaussian matrix. Non-linear conjugate gradient algorithm (NCGM) [17] and fast Fourier transform (FFT) [11–15] have been popularly adopted in this step.

In our simulation of the non-Gaussian surfaces, the ACF is expressed as:

$$R = \exp\left[-\left\{\left(\frac{t_x}{b_x}\right)^2 + \left(\frac{t_y}{b_y}\right)^2\right\}^{\omega}\right] \quad (1)$$

Here, t_x and t_y are lags in the x and y directions, respectively. b_x and b_y are the correlation lengths in the x and y directions, respectively. Parameter ω expresses the degree of mixture of the long wave component and short wave component. FFT method is also adopted in our simulation process because it is simple and highly efficient.

2.2. Comparison of simulations based on Johnson translator and Pearson translator

We mainly focus on the comparisons of roughness surface generation based on Johnson translator and Pearson translator. Parameter ω mentioned above is chosen as 1. From theoretical analysis, the parameters skewness and kurtosis, which are inputted to Johnson translator and Pearson translator in module B, must fulfill the following relation [13]:

$$Ssk^2 - Sku + 1 \leq 0 \quad (2)$$

where Ssk and Sku represent skewness and kurtosis. Fig. 2 verifies the theoretical relation. The square points in Fig. 2(a) illustrate that Johnson translator is fit for the input parameters represented by corresponding coordinate values. Similarly, Fig. 2(b) illustrates the application range of Pearson translator. Small crosses in the two figures illustrate that the corresponding input parameters are not suitable for the translators. The curves in the figures represent $Ssk^2 - Sku + 1 = 0$. Some boundary points do not comply well due to digitization, and they can be ignored. Results show that both translators can achieve conversion from a Gaussian matrix to a non-Gaussian matrix, and the simulation results agree well with the theoretical analysis. In some individual boundary points, Johnson translator performs better.

After verifying the selectable range of the input parameters of the two translators, we analyze the influence of correlation length when three simulation modules integrated together. Fig. 3

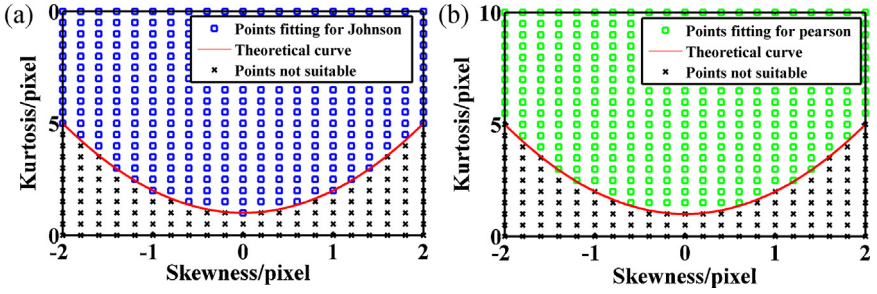

Fig. 2. Comparison of the two translators. (a) The parameter range fitting for Johnson translator. (b) The parameter range fitting for Pearson translator.